Ultrasonic

by Ultrasonic Ultrasonic

Submission date: 01-Apr-2023 10:08PM (UTC+0700)
Submission ID: 2052874299
File name: 2023_Ultrasonic_irradiation.pdf (5.57M)
Word count: 6249
Character count: 33226

South African Journal of Chemical Engineering 43 (2023) 359–368

Contents lists available at ScienceDirect

South African Journal of Chemical Engineering

journal homepage: www.elsevier.com/locate/sajce

Ultrasonic irradiation as a mild and efficient protocol for the demineralization of chitin from shrimp shell wastes

Nufus Kanani [a], Teguh Kurniawan [a,d], Widya Kosimaningrum [a], Yenny Meliana [b], Jayanudin [a], Endarto Wardhono [a,c,*]

[a] Chemical Engineering Department, University of Sultan Ageng Tirtayasa, Jl. Jendral Sudirman Km 3, Cilegon 42435, Indonesia
[b] Research Center for Chemistry, National Research and Innovation Agency, BRIN, Kawasan Puspiptek, Banten 15314, Indonesia
[c] Laboratorium Polimer dan Komposit, Centre of Excellent, University of Sultan Ageng Tirtayasa, Jl. Jendral Sudirman Km 3, Cilegon 42435, Indonesia
[d] Laboratorium Valorisasi Biomassa, Centre of Excellent, University of Sultan Ageng Tirtayasa, Jl. Jendral Sudirman Km 3, Cilegon 42435, Indonesia

ARTICLE INFO

Keywords:
Shrimp shell wastes
Chitin
Demineralization
Ultrasonic irradiation
Simple decomposition model

ABSTRACT

Chitin is conventionally isolated under harsh reaction conditions through two constitutive steps deproteinization and demineralization. This paper considers a protocol for chitin's isolation from shrimp shell waste. Ultrasonic irradiation was employed as an effective technique for the isolation process at a mild reaction condition with dilute solvents, a lower temperature and shorter reaction times compared to the conventional one. Shrimp shells wastes were pretreated by washing, grinding and sieving. The grounded shells were deproteinized with 2 M sodium hydroxide solution and followed by demineralization using 1 M hydrochloric acid. The mechanisms by which the demineralization occurs in the deproteinized shells were described using a simple decomposition model. Quantitative mineral analysis was performed by titrimetric at different temperatures 40, 50, 60, and 70 °C under constant ultrasound power and frequency. The results indicated that the protein content significantly reduced to 0.87% w/w when the highest NaOH concentrations were reached. At the same time, the ultrasound assists demineralization, resulting in the lowest mineral content of 1.29% w/w. This work also effectively demonstrates the kinetic model that occurs through the demineralization, in which reaction rate, $\frac{dCaCO_3}{dt} = -k_2\frac{K_1 C_{CaCO_3}}{(1+2K_1 C_{CaCO_3})}$ and $k_2 = Ae^{-\frac{E_a}{RT}}$ are an excellent model to describe the process. In this work, the physicochemical characterization showed that the properties of isolated chitin were not much influenced by the ultrasonic treatment, which has the same characteristics as the commercial product.

1. Introduction

Chitin is the most available amino-polysaccharide in nature. It is a nitrogenous compound commonly found in organisms such as crustacean shells, insect cuticles, fungi, and alga cell walls (Borić et al., 2020; Santos et al., 2020). Chitin is arranged as ordered microfibrils embedded in a complex network to form a natural matrix with protein and minerals. Resemble with cellulose in structural and functional, and chitin is a linear chain molecule consisting of (1–4)−2-acetamido-2-deoxy-b-D-glucan repeating unit (Oyekunle and Omoleye, 2019), which serves as supportive components to support the exoskeletons of crustaceans, whereas cellulose contributes to the strength of plants (Gooday, 1990). Chitosan is one of the most important chitin derivatives, generally obtained from partial or total deacetylation of chitin (Wardhono et al., 2021). Chitosan is well known as a versatile material with high economic benefits due to its excellent properties such as nontoxicity, biodegradable and biocompatible that have been widely used in biomedical (Hu et al., 2021), food (Jovanović et al., 2021), cosmetics (Ta et al., 2021), and wastewater treatment (Wang et al., 2021).

The primary sources of chitin for commercial applications are marine crustacean shells, especially shrimps and crabs. They have the highest content compared to other sources consisting of 20–30% chitin, 25–35% protein, and 30–40% calcium carbonate (Alabaraoye et al., 2018). Chitin is generally isolated by two-process constitutive: (1) thermo-alkaline method to disrupt the proteins; (2) and acidic treatment to remove minerals, mainly calcium carbonate, $CaCO_3$. Chemical deproteinization is carried out using 1–5 M aqueous sodium hydroxide (NaOH) solutions at temperatures up to 160 °C until 72 h (Percot et al.,

* Corresponding author at: Chemical Engineering Department, University of Sultan Ageng Tirtayasa, Jl. Jendral Sudirman Km 3, Cilegon 42435, Indonesia.
E-mail address: endarto.wardhono@untirta.ac.id (E. Wardhono).

https://doi.org/10.1016/j.sajce.2022.12.004
Received 3 August 2022; Received in revised form 5 December 2022; Accepted 21 December 2022
Available online 29 December 2022

2003). It is a tough process because chitin forms a complex link with proteins in the solid shells. For biomedical applications, complete protein removal is needed because of allergy-causing protein issues in some people. Chemical demineralization is generally performed using strong acid solvents such as hydrochloric acid (HCl), nitric acid (HNO_3), and sulfuric acid (H_2SO_4). Among these reagents, the preferential is HCl, carried out under stirring with the following conditions: 0.5–2 M, time ranges from 1 to 48 h, and reaction temperature up to 100 °C. It undergoes the decomposition of $CaCO_3$ into the water-soluble calcium salt with the release of CO_2 as the following equation (Younes and Rinaudo, 2015):

$$2HCl_{(aq)} + CaCO_{3\,(s)} \rightarrow CaCl_{2\,(aq)} + H_2O_{(l)} + CO_{2\,(g)} \quad (1)$$

The $CaCl_2$ salt is then removed from the product by washing using deionized water. It is an empirical process that depends on the raw shell sources and extraction conditions such as time, temperature, particle size, type, acid concentration, and solute/solvent ratio. However, chemical demineralization is high energy consumption, and the solvent used is corrosive, which causes pollution from soils to plants and animals. Moreover, the harsh reaction conditions induce depolymerization, resulting in inconsistent physiological properties in the end product (Paul et al., 2015).

The growing demand for a green and sustainable technology for isolation chitin with minimum product degradation, less solvent used, energy-saving processes, and limiting wastes has attracted many researchers. An alternative technique could be an ultrasound wave that presents faster kinetics in the operating temperature and higher yield in recovering thermolabile substances (Patel et al., 2019). Ultrasonics represent mechanical waves by generating longitudinal acoustic waves over 18 kHz, which are still higher than the human hearing thresholds below 16 kHz. The high-intensity sound waves impose local vibration of particles in a solid medium and acoustic cavitation in a liquid medium (Yao et al., 2020). Acoustic cavitation is the oscillation and explosion of millions of air bubbles in the water. It induces extreme conditions and generates vastly reactive radicals in which a chemical reaction cannot occur in a normal condition (Ashokkumar, 2011). Ultrasound-wave has been widely applied in the process intensification, including the synthesis of nanomaterials (Wardhono et al., 2018), biopolymer composites (Wardhono et al., 2019; Pinem et al., 2020), organic degradation (Wang et al., 2019), emulsification (Zhang et al., 2020), cleaning (Aktij et al., 2020) etc. Compared to other novel techniques, microwave-assisted extraction, for example, ultrasound, is cheaper and more accessible. It can be used for a small amount of material and minimize the expenditure of solvents. The challenges faced in large-scale applications are designing specific power ultrasonic systems. So investigating the reaction kinetics from the mineral deposition is essential to optimizing and understanding the process.

This work develops a simple and efficient technique for chitin isolation under ultrasound waves. Acoustic cavitation is hypothesized to improve the process by enhancing the leaching of protein contents and intensifying mineral reduction. The protocol produces higher yields within a low temperature and short time. It is a potential tool to decrease energy supplies and act as a processing protocol with less solvent consumption than the conventional process. The study highlights determining kinetic parameters representing mineral content reduction occurring in the solid shell particle and obtaining the best protocol of $CaCO_3$ removal compared to the conventional method. The reaction was carried out in an ultrasound-assisted batch reactor at constant power and frequency. The protein content was eliminated previously from the raw shells using an aqueous NaOH solution at a warm temperature. The mineral calcium reduction was conducted in a dilute hydrochloric acid liquid media, in which the complexometric titration was used to determine the $CaCO_3$ residues from the matrix structure of the deproteinized powder. The kinetic data for the effects of various reaction conditions were investigated and fitted by a simple decomposition model. To the best of our knowledge, it is the first to report the kinetics of the demineralization of shrimp shells using this model. The physicochemical properties of the isolated chitin were then characterized by Fourier Transform Infra-Red (FTIR) spectroscopy for chemical structure identification, X-ray fluorescence (XRF) for elemental analysis, gel permeation chromatography (GPC) for molecular weight determination, X-Ray Diffraction (XRD) for crystallinity index calculation, Differential Scanning Calorimetry (DSC) for thermal behavior characterization, and Scanning electron microscopy (SEM) for surface morphology. The Physicochemical properties of the obtained product were then compared to the commercial one.

2. Experimental

Shrimp shells were collected from a local market in Serang (Banten, Indonesia) region. Lab-grade chemicals, NaOH, and HCl were purchased from Merck Indonesia (Jakarta, Indonesia). Distilled water and reagents such as solid Ethylene Diamine Tetra Acetic acid (EDTA), Eriochrome Black T (EBT) indicator, buffer pH 10, HNO_3 and H_2SO_4 were supplied from a local chemical supplier.

2.1. Raw shell preparation

The wet shells were soaked in dilute NaOH solution 0.25% (w/v) at room temperature for 2 h and washed in tap water to remove lipids, adhere protein, excess tissues, and dirt. The clean shells were rinsed with distilled water before being sun-dried for seven days. The dried shells were ground using a kitchen blender, sieved through 100 Mesh, and kept in a sealed container before preparation.

2.2. Ultrasonic treatment

The ultrasonic device (Vibra-Cell 72,434, 100 W, Ø: 1.0 mm) was set to 20 kHz and amplitude 100%. The irradiation was carried out directly the material by immersing the ultrasonic probe at the suspension's midpoint, constantly stirring and heating using a hot plate magnetic stirrer.

Deproteinization (with a solid-to-liquid ratio of 1:10) was performed by introducing the ground shell into 100 mL of NaOH solution (0 – 2 M) into a 200-mL flat-bottom flask with jointed necks to circulating water condenser, while the temperature was controlled at 60 °C, stirring speed 200 rpm for 1 h. After the treatment, the desired product was discharged from the liquid, washed with drain water until neutral, and oven-dried at 70 °C overnight before characterization and further preparation.

After deproteinization, 10% w/v of dried deproteinized shells were ultrasound-assisted demineralized with 100 mL of HCl solution at the reaction temperatures (40; 50; 60; 70 °C) for up to 1 h to prepare chitin. The end products were overnight oven-dried at 70 °C and analyzed using complexometric titration to determine the number of calcium ions degraded with hydrochloric acid.

2.3. Characterization

2.3.1. Kjeldahl method

1 g of sample was hydrolyzed with 20 mL concentrated H_2SO_4 (98% w/v) containing 2 g of selenium at a temperature of 350 °C and allowed to stand for 4 h. After cooling to room temperature, the hydrolysates were diluted with distilled water up to 100 mL, neutralized with 50 mL NaOH (50% w/v), and then transferred to the distillation unit. 150 mL of the condensate was received in a 250-mL Erlenmeyer flask containing 50 mL of KCl solution (0.1 M) and then titrated with HCl 0.1 M until the solution had a pink color. The protein content was calculated by multiplying the total HCl needed with a conversion factor of 6.25.

$$\%\text{Protein} = \frac{(a-b)\ \text{x N x } 14.00}{W_s(1000)}\ \text{x } 100\ \times\ 6.25 \quad (2)$$

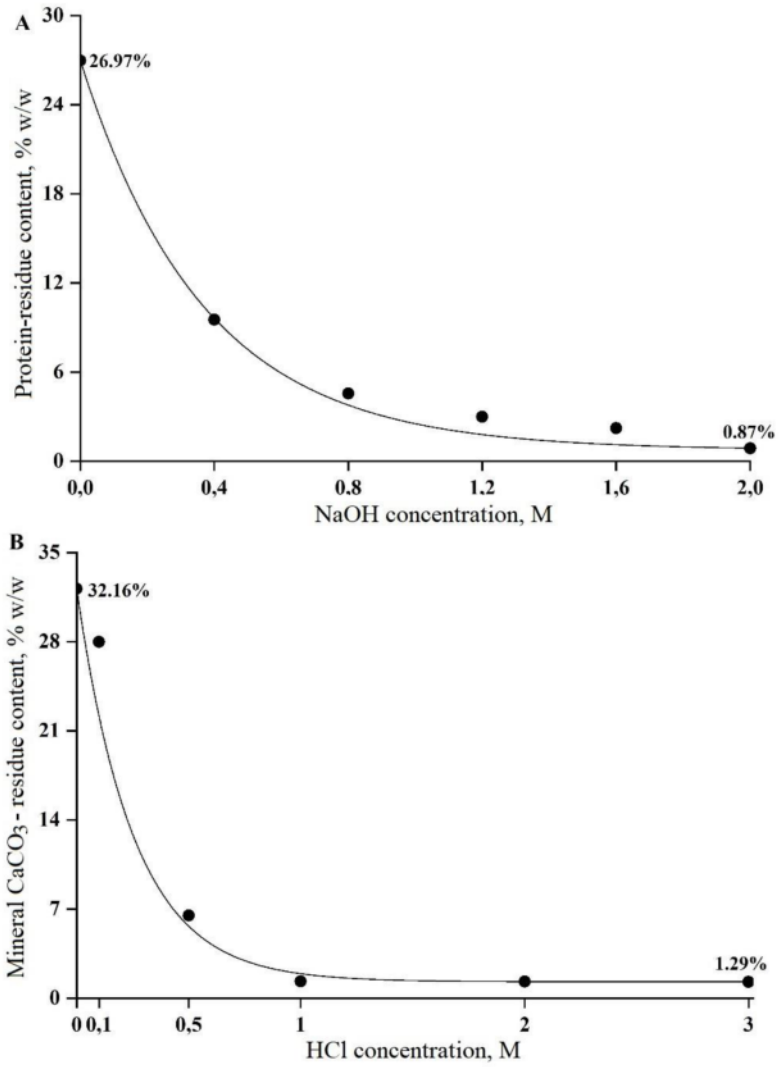

Fig. 1. Effect of ultrasonic treatment on: deproteinization of the grounded shrimp shells at difference NaOH concentrations (A); demineralization of the deproteinized shells at difference HCl concentrations (B).

where a = Volume (ml) of the sample's titration
b = Volume (ml) of the control's titration
N = concentration of HCl
Ws = Sample weight
14 = atomic weight of Nitrogen

2.3.2. Titrimetry

10 mL of an aliquot sample solution was prepared by dissolving 0.5 g of the sample product in an Erlenmeyer flask 25-mL containing a mixture of 5 mL of dilute H_2SO_4 (10% w/v) and 5 mL of dilute HNO_3 (10% w/v) at room temperature and stirred with a magnetic stirrer for 10 min. 1 mL of the sample solution was transferred to a 100-mL Erlenmeyer flask and diluted with distilled water to 100 mL of total volume solution. 10 mL diluted aliquot of the sample solution were pipetted into a 100-mL Erlenmeyer flask. 0.1 g of EBT indicator and 1 mL of buffer solution (pH-10) were added to the diluted aliquot and allowed to stand for about 5 min with occasional swirling. The sample was titrated with the EDTA solution until the color changed from pink to blue. The titration was repeated until concordant results were obtained. The measurements were repeated three times, and the data presented here fall under the 95% confidence interval.

2.3.3. FTIR

The functional groups present in the samples were identified using Nicolet iS5 spectrometry (Thermo Scientific, Waltham, MA, USA). The sample pellets were prepared using the KBr method, in which the absorption bands were scanned from 4000 to 400 cm^{-1}.

2.3.4. XRF

Elemental analysis was conducted to detect various elements in the sample products by XRF Bruker S2 PUMA ((Bruker, MA, USA). The spectrometer has a detector optimized for light element detection and contains a 50 keV and 50 mA X-ray tube.

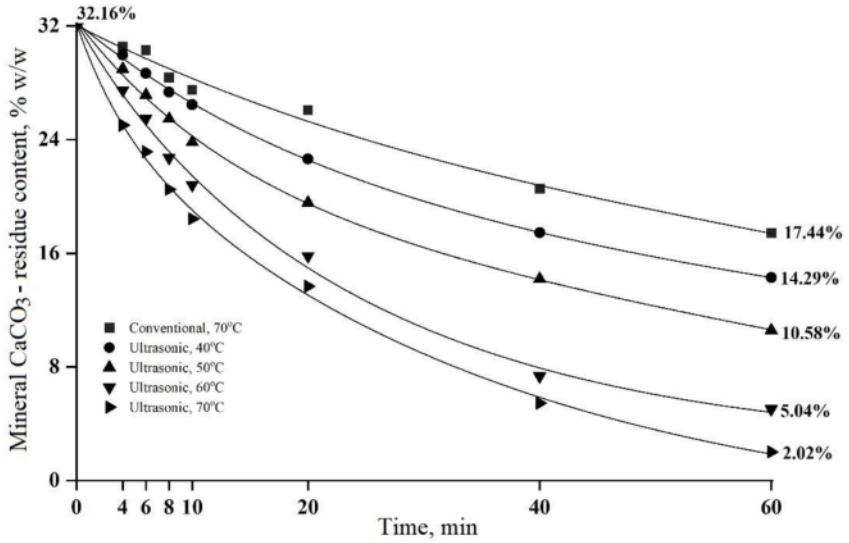

Fig. 2. Effect of ultrasonic treatment on the depletion of $CaCO_3$ in the shrimp shells .

2.3.5. GPC

Molecular weight, Mw determination was performed using a Shimadzu GPC system, LC-10AVP/LC-10ADVP instrument (Shimadzu, Tokyo, Japan). 20 µl of 0.5% chitin solutions in 5% N, N-dimethylacetamide/lithium chloride (DMAc/LiCl) was injected system at 40 °C. The measurement was calibrated with pullulan standards.

2.3.6. XRD

The XRD patterns were recorded on D8 Advance (Bruker, MA, USA) with CuKα radiation, operating at 40 kV and 50 mA, and scanning rate at $1°.min^{-1}$, in which the deconvolution method was used to calculate the crystallinity index (CrI) (Park et al., 2010).

$$CrI = \frac{A_{Cr}}{A_{tot}} x100\% \quad (3)$$

where A_{cr} = area of the crystalline curves

A_{tot} = total area of the curve

2.3.7. DSC

The temperature decomposition of the samples was characterized using TGA-Q50 (Shimadzu, Japan). 5 mg samples were heated from ambient temperature to 800 °C with a heating rate of 25 °C/min.

2.3.7. SEM

The surface morphologies of the micro-crystalline samples were visualized using JEOL-2100F (JEOL Ltd., Japan) at a magnification of 1000x. The sample was deposited on the sample holder and coated with carbon support.

3. Results and discussions

3.1. Effect of ultrasonic treatments

Deproteinization of the grounded shrimp shells was performed under ultrasonic irradiation immersed in the various concentrations of NaOH solutions prior to demineralization. The results of the Kjeldahl analysis are presented in Fig. 1A. The figure shows the decrease of the protein-residue content as a function of NaOH concentration in the grounded shells. Under 1 h of reaction at 60 °C, the protein residue significantly reduced up to 0.87% w/w when the highest NaOH concentrations reached 2 M, from the initial value of 26.97% w/w. An increase in the solvent concentration improves the leaching of proteins fortified by ultrasonic waves. The vibration effects of the ultrasonic wave produce cavitation phenomena in the solvent (Görgüç et al., 2019) that induce the breakage of nitrogen bonds and degrade the protein content.

The mineral fractions, primarily $CaCO_3$, were eliminated from the deproteinized shells via acid treatment, which resulted in soluble salt, $CaCl_2$, and chitin leaving them as insoluble matter. Demineralization was carried on for 1 hour at 60 °C under an ultrasound-assisted isolation procedure at different HCl concentrations ranging from 0.01 to 3 M. The results of the titration method are shown in Fig. 1B. The ultrasound assists demineralization as acid concentration reduces from 32.16% to 1.29% w/w. The reaction dynamics are significantly affected by acid solvent concentration. For the lower concentration of 0.01–1 M, the $CaCO_3$-residue content decreases rapidly for 60 min of the reaction. Then the reduction of the mineral content tends to be constant as the higher concentration of 1–3 N at the same period of reaction. It is observed that the optimum HCl concentration is 1 M at a much lower mineral reduction rate compared to the others. The sonication during the process decreases the amount of mineral content that improves reaction efficiency (Peshkovsky and Peshkovsky, 2010). Acoustic cavitation causes extremes of temperature and pressure in liquid media. It increases mass diffusivity in a solid medium and promotes the mass transfer process (Yao, 2016).

3.2. Kinetic study of demineralization

The ultrasonic-assisted demineralization was then performed at the optimum acid concentration (1 M) with temperatures ranging from 40 to 70 °C and compared to a standard demineralization process at 70 °C. A gradual depletion of $CaCO_3$ in the shrimp shells is presented in Fig. 2.

The Figure shows the reduced mineral content of the shrimp shells at each sampling point. The minimum $CaCO_3$ level ~~is~~ was achieved at 14.29% (40 °C), 10.58% (50 °C), 5.04% (60 °C), and 2.02% (70 °C) from the initial value 32.16% after 60 min of the treatment. The conventional result gives a higher value (17.44% for 70 °C) than the ultrasonic method in all temperature variables. In this case, the formation of CO_2 resulted in a foaming form. Solid-phase demineralization is a complex process involving multiple chemical reactions and mass transfer steps. The reaction rate may depend on many factors, including particle size,

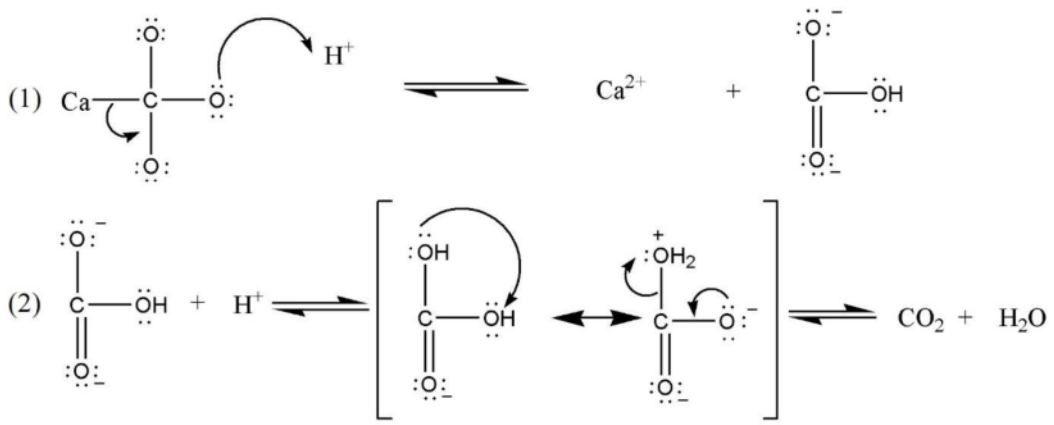

Fig 3. Mechanism reaction of $CaCO_3$ demineralization.

surface area, pH, stirring speed, temperature, and pressure (Baron et al., 2015). The reaction mechanisms involve two steps: (1) acid dissolves mineral due to H^+ protonate the carbonic oxygen group that induces the dissociation of Ca^{2+} and formation of bicarbonate ion, HCO_3^-; (2) the bicarbonate, HCO_3^-receives another proton to yield carbonic acid, H_2CO_3 that is decomposed immediately to water, H_2O and the volatile gas, CO_2 (Fusi et al., 2012) (Fig. 3).

The mathematical model represents kinetic reactions associated with mineral content solubilization under ultrasonic treatment are investigated through a simple decomposition model fitted from the experimental data. According to Alkhaldi et al. (2010), the basic equation of the mineral decomposition reaction between the acid solvent and calcium carbonate is presented as follows.

$$2H^+ + 2Cl^- + CaCO_{3\,(s)} \leftrightarrow {}^{k_1}{}_{k_{-1}} CaCl^+ + Cl^- + H_2O_{(l)} + CO_{2\,(g)}\uparrow \tag{4}$$

k_1 = The forward reaction-rate constant at the initial reaction, k_{-1} = The reverse reaction-rate constant at the initial reaction,

The formation of $CaCl_2$ has affected the equilibrium reaction of HCl with $CaCO_3$. Due to calcium chloride being partially depleted, the equilibrium reaction will shift toward the products.

$$CaCl^+ + Cl^- \xrightarrow{k_2} CaCl_{2\,(aq)} \tag{5}$$

k_2 = The reaction-rate constant at the final reaction,

Suppose it is assumed that the concentration H^+ is uniform in the bulk solvent, while $CaCO_3$ content changes with time. The equation for the equilibrium is given by:

$$k_1(C_{H^+})^2 C_{CaCO_3} = k_{-1} C_{CaCl^+} \tag{6}$$

Based on HCl mass-conservation considerations;

$$C_{H^+,0} = C_{H^+} + C_{CaCl^+} \tag{7}$$

$$\text{Or,}\ \ C_{H^+} = C_{H^+,0} - C_{CaCl^+} \tag{8}$$

Using Eqs. (9) to (7), this may be written

$$k_1\left(C^2_{H^+,0} - 2C_{H^+,0}C_{CaCl^+} + C^2_{CaCl^+}\right)C_{CaCO_3} = k_{-1}C_{CaCl^+} \tag{9}$$

To simplify the equation, $C_{CaCl^+} \ll C_{H^+,0}$, hence we may eliminate the term $C^2_{CaCl^+}$

$$k_1\left(C^2_{H^+,0} - 2C_{H^+,0}C_{CaCl^+}\right)C_{CaCO_3} = k_{-1}C_{CaCl^+} \tag{10}$$

$$k_1 C^2_{H^+,0} C_{CaCO_3} - 2k_1 C_{H^+,0} C_{CaCl^+} C_{CaCO_3} = k_{-1} C_{CaCl^+} \tag{11}$$

$$k_1 C^2_{H^+,0} C_{CaCO_3} = 2k_1 C_{H^+,0} C_{CaCl^+} C_{CaCO_3} + k_{-1} C_{CaCl^+} \tag{12}$$

$$k_1 C^2_{H^+,0} C_{CaCO_3} = \left(2k_1 C_{H^+,0} C_{CaCO_3} + k_{-1}\right) C_{CaCl^+} \tag{13}$$

$$C_{CaCl^+} = \frac{k_1 C^2_{H^+,0} C_{CaCO_3}}{\left(k_{-1} + 2k_1 C_{H^+,0} C_{CaCO_3}\right)} \tag{14}$$

The formation rate of the product, $CaCl_2$ can be written:

$$r_{CaCl_2} = k_2 C_{CaCl^+} \tag{15}$$

$$r_{CaCl_2} = k_2 \frac{k_1 (C_{H^+,0})^2 C_{CaCO_3}}{\left(k_{-1} + 2k_1 C_{H^+,0} C_{CaCO_3}\right)} \tag{16}$$

$$r_{CaCl_2} = k_2 \frac{K_1 (C_{H^+,0})^2 C_{CaCO_3}}{\frac{1}{k_{-1}}\left(\frac{k_1}{K_1} + 2K_1 k_{-1} C_{H^+,0} C_{CaCO_3}\right)} \tag{17}$$

$$r_{CaCl_2} = k_2 \frac{K_1 (C_{H^+,0})^2 C_{CaCO_3}}{\left(\frac{k_1}{k_{-1}K_1} + 2K_1 C_{H^+,0} C_{CaCO_3}\right)} \tag{18}$$

$$r_{CaCl_2} = k_2 \frac{K_1 (C_{H^+,0})^2 C_{CaCO_3}}{\left(\frac{K_1}{K_1} + 2K_1 C_{H^+,0} C_{CaCO_3}\right)} \tag{19}$$

$$r_{CaCl_2} = k_2 \frac{K_1 (C_{H^+,0})^2 C_{CaCO_3}}{\left(1 + 2K_1 C_{H^+,0} C_{CaCO_3}\right)} \tag{20}$$

Substitute, $K_1 = \frac{k_1}{k_{-1}}$, where K_1 is equilibrium constant for the initial reaction

$$r_{CaCl_2} = k_2 \frac{K_1 (C_{H^+,0})^2 C_{CaCO_3}}{\left(1 + 2K_1 C_{H^+,0} C_{CaCO_3}\right)} \tag{21}$$

If the reaction time required to form $CaCl_2$ equals to demineralize of $CaCO_3$

$$r_{CaCO_3} = -r_{CaCl_2} \tag{22}$$

$$\frac{dCaCO_3}{dt} = -k_2 \frac{K_1 (C_{H^+,0})^2 C_{CaCO_3}}{\left(1 + 2K_1 C_{H^+,0} C_{CaCO_3}\right)} \tag{23}$$

In our experiment $(C_{H^+,0}) = 1M$

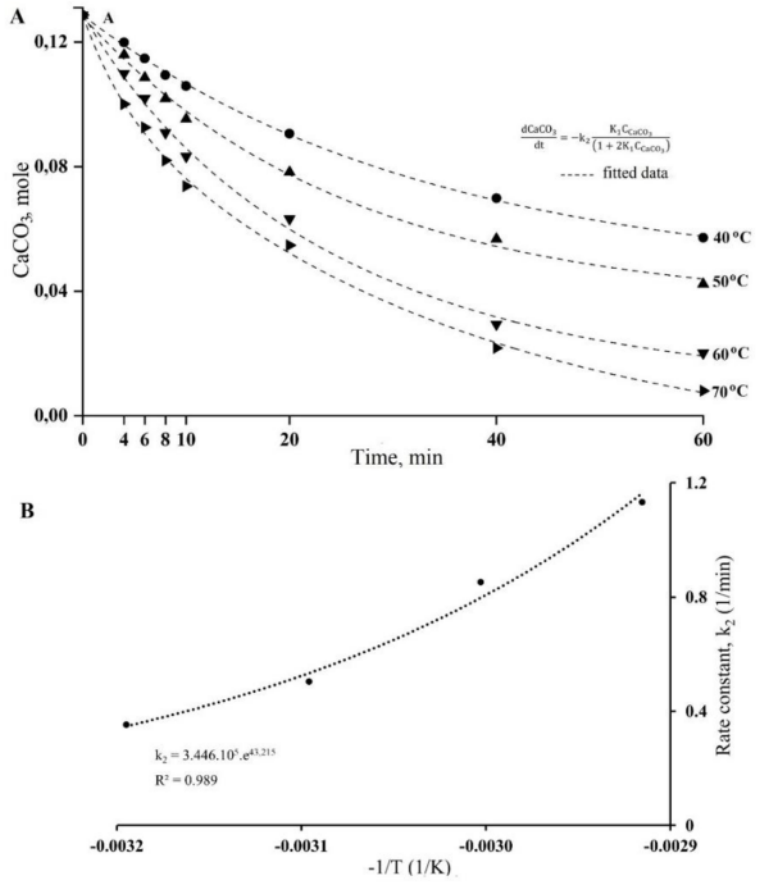

Fig. 4. Kinetic model of deminarlization $CaCO_3$ content in the shrimp shells under ultrasound wave (A); Arrhenius equation data (B).

Table 1
Kinetic parameters of demineralization reaction $CaCO_3$ content in the shrimp shells under ultrasound irradiation.

Temp (°C)	k_2 (1/min)	K_1	Reaction order	Arrhenius parameters
40	0.353	4.524×10^{-2}	1	$A = 3.447 \times 10^5$
50	0.504			
60	0.853			Ea = 359.289
70	1.132			

$$\frac{dCaCO_3}{dt} = -k_2 \frac{K_1 C_{CaCO_3}}{(1 + 2K_1 C_{CaCO_3})} \quad (24)$$

Using the modeling Eq. (24), non-linear graphs for each temperature treatment are plotted, as shown in Fig. 4.

Fig. 4A shows the depletion concentration of $CaCO_3$ with the time of the experimental data, along with the fitting curves of each temperature model. The model was fitted by a simple decomposition model, being better at a lower temperature ($R^2 = 0.999$ at 40 °C and $R^2 = 0.998$ at 50 °C), while the higher one produces discrepancies slightly ($R^2 = 0.996$ at 60 °C and $R^2 = 0.997$ at 70 °C). The correlation coefficient (R^2) values for all the models considered demonstrate that they are good at predicting the reaction mechanism in the shrimp shells. At the same time, an empirical equation using the Arrhenius equation presents the dependence of rate constants on temperature.

$$k_2 = Ae^{-\frac{E_a}{RT}} \quad (21)$$

k_2 = the rate constant R = the universal gas constant, J/mol.K
A = the pre-exponential factor. T = Absolute temperature, K
Ea = the activation energy, J/mol

Parameters estimation in kinetic models of solid-phase demineralization under ultrasound wave is listed in Table 1. The values obtained, considering that the molar concentration of the reactant, HCl, is constant at 1 M throughout the reaction.

The Arrhenius equation is the empirical model to describe the relationship between reaction rate and temperature from experimental data. Fig. 5B shows an Arrhenius plot of the rate constant, k_2 versus $-1/T$. The slope calculated from the curve yields the pre-exponential factor, $A = 3.447 \times 10^5$ and the activation energy, Ea = 359.289 J/mol. It observes that the validity of the Arrhenius equation is a significantly higher accuracy obtained $R^2 = 0.989$.

3.3. Characterization of chitin

Following the previous results, in this part, the impact of ultrasound-assisted extraction on the physiochemical characteristics of isolated chitin is evaluated and compared with the commercial one.

FTIR identification was performed to identify the chemical structure of the isolated chitin compared to the commercial product. The IR bands of the samples are shown in Fig. 5A, and typical vibration bands are

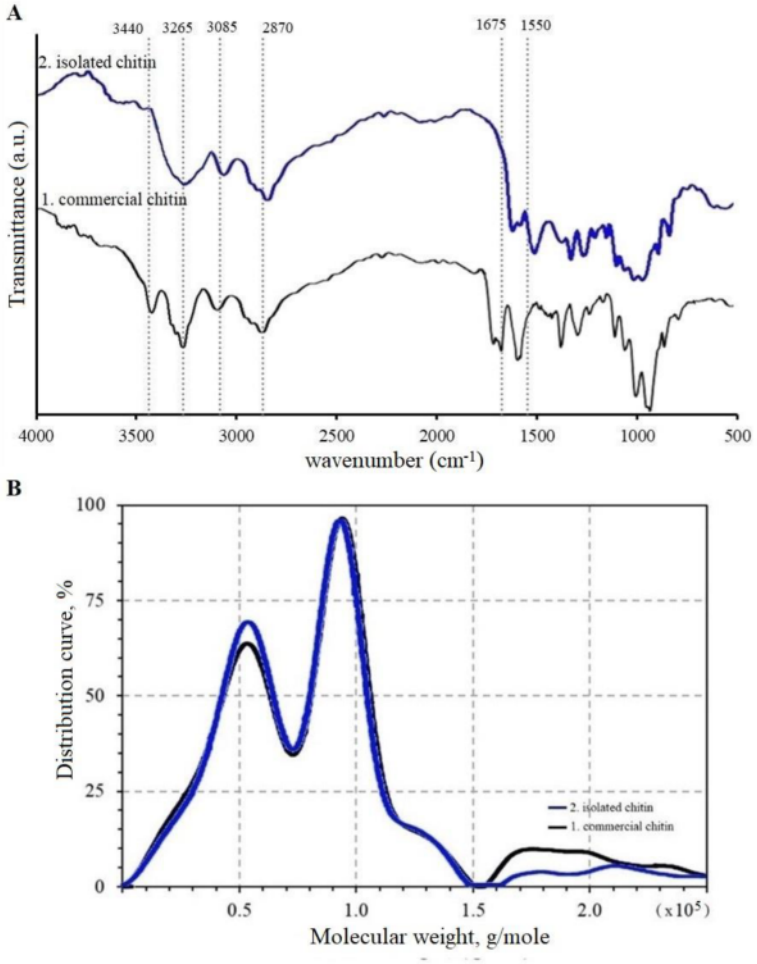

Fig 5. Characterization of chitins: FTIR spectra (A); GPC chromatogram (B).

Table 2
Typical vibration bands of the chitin (Liu et al., 2012).

Wave number (cm-1)	Functional groups
3440	ν (O—H)
3265; 3085	ν (N—H)
2870	ν (C—H)
1675	ν (C—O)
1550	δ(N—H)

listed in Table 2.

The characteristics of biopolymer chitin are specified by `the absorption bands at 1550 and 1675 cm^{-1} that represent the amide I of C = O stretching vibration. The absorption bands at 3085 and 3265 cm^{-1} correspond to the amide II band of N—H bending in N-acetyl groups. The configuration at 2870 cm^{-1} can refer to C—H vibration, and the weak band at 3440 cm^{-1} is linked to the O—H stretch. The spectra show that the isolated chitin (in blue line) is comparable to the commercial one (in black line), which covers vibrational fingerprints at the same points. However, some bands were slightly changed. It indicates that rearrangements on the polymeric chain occurred during the ultrasonic treatment.

Table 3
Elemental analysis of chitin.

Sample	Organic matter,% (w/w)			C/N	DA,%
	C	H	N		
Isolated chitin	41.47	6.45	6.29	6.59	84.5
Commercial chitin	43.73	6.92	6.57	6.66	88.1

The elemental analysis was carried out to get the C/N ratio to calculate the DA of the samples. It is a destructive method to determine the organic matter composition of the chitins. The elemental carbon, C, hydrogen, H, nitrogen, and N content obtained are presented in Table 3. The following formula determines the degree of acetylation (DA) in the samples (Xu et al., 1996).

$$DA(\%) = \left[\frac{C/N - 5.14}{1.72}\right] x100 \quad (22)$$

Where C/N is ratio of carbon to nitrogen.

The N content is 6.29% and 6.57% for the isolated chitin and the commercial product, respectively. These come from protein residue and chitin in the sample analyzed. The results measured are less than the theoretical value of total nitrogen content (6.89%) for fully acetylated

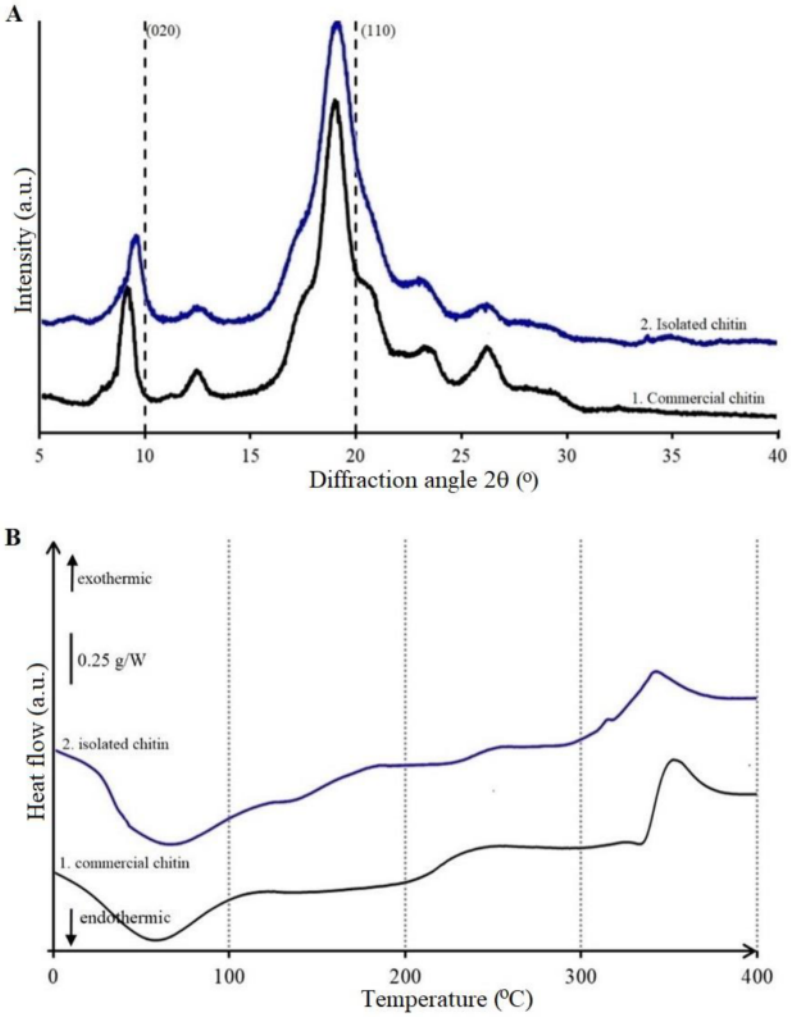

Fig. 6. Characterization of chitins: XRD pattern (A); DSC thermogram (B).

chitin (Kaya et al., 2017). The values suit using the Kjeldahl method, in which the N content is 6.22% for isolated chitin and 6.51% for commercial chitin. In this work, the DA value of commercial chitin measured is 88.1%, while the DA of the isolated chitin is 84.5%. The irradiation is not much influenced by the DA irradiation, which remains in the range of 84 - 88%.

Mw of all chitin samples was measured by GPC using pullulan as standard. As predicted, both chitins give a similar pattern in the chromatogram profiles, as shown in Fig 6A. The Mw of the isolated chitin is 1068×10^3 g/mole is somewhat similar to the Mw of the commercial one, which is 1156×10^3 g/mol. The difference could be explained by its lower DA, namely 84.5%.

XRD analysis was employed to determine the chitins' crystallinity degree. It is a non-destructive technique that provides accurate information to identify a crystalline structure present in a polymer. Fig. 6A presents the diffractogram of the commercial chitin and the chitin extracted using ultrasound irradiation.

The XRD pattern of the isolated chitin (in blue line) exhibits two high-intensity peaks at diffraction angle 9.3° and 19.4°, and four low-intensity peaks at 2θ = 12.8°, 20.8°, 23.5° and 26.4°, which represent crystalline polymorphs (Knidri et al., 2019; El Knidri et al., 2016). The pattern is similar to peak positions determined for the commercial chitin (in black line). These results are in agreement with previous reports in which the prominent peaks of the chitin crystalline region were identified at diffraction angles at ~10° and ~20° (Majekodunmi, 2016; Ahyat et al., 2017; Hahn et al., 2020). The crystallinity values value is calculated using Eq. (3), in which the CrI of commercial chitin is obtained at 68.5% and 66.0% for isolated chitin. In this case, the crystal structure of isolated chitin was not destroyed by the ultrasound wave while maintaining the crystallinity close to the commercial one.

The DSC test studied the thermal property, in which the thermal stability of chitins was determined to describe the temperature decomposition of materials during heating. Fig. 6B shows the DSC thermograms of the samples. Compared to the commercial chitin, the isolated one shows a relatively similar pattern as the sample heated from 0 to 400 °C. The endothermic peak is detected around 65 °C, which is related to the loss of water content in the material. While the exothermic peak appears in the temperature range of about 330 and 380 °C corresponds to the thermal decomposition of the chitin (Pereira et al., 2013).

SEM images were recorded to evaluate the morphological changes on

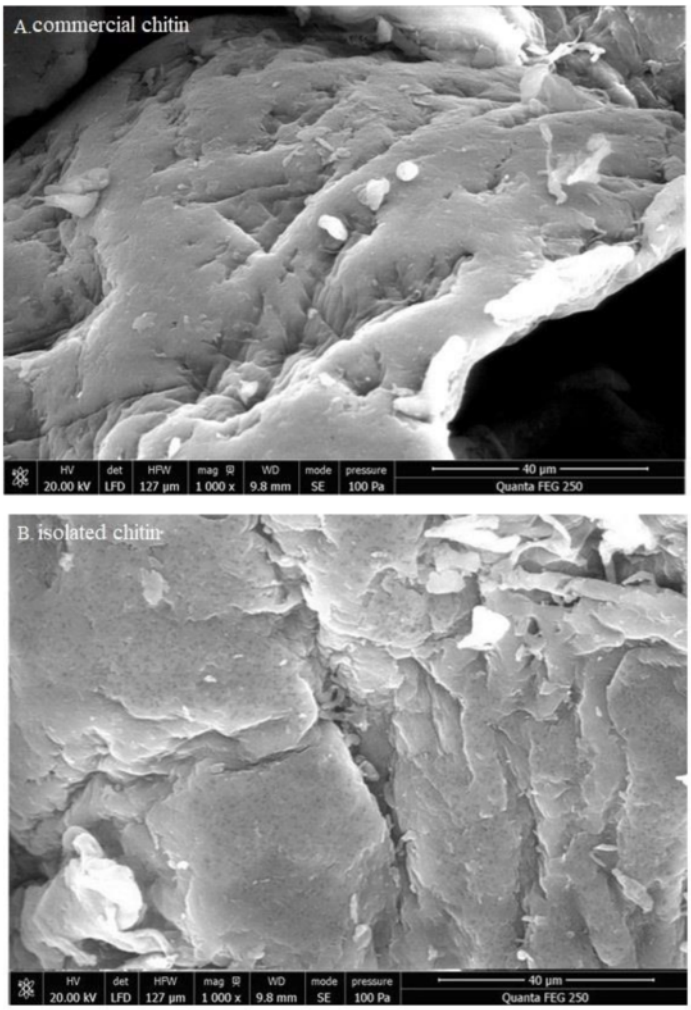

Fig. 7. SEM images of: commercial chitin (A); isolated chitin (B).

the polymer surface caused by the ultrasound procedure. The images are presented in Fig. 7.

Fig 7 shows commercial chitin has a smooth and solid surface, while the isolated chitin displays a rough and fracture surface. It is also observed that some parts of the isolated sample shows small holes in the surface due to sonication's cavities effects.

4. Conclusions

Ultrasonic irradiation was employed as a mild protocol for chitin's isolation from shrimp shell wastes. Irradiation appears as a simple technique to improve the efficiency of extraction procedures without any significant destruction to the product's structure. The series of characterization indicated that the isolated product has the same characteristics as the commercial chitin. The FTIR spectra show that the isolated chitin has a similar chemical structure to the commercial one which shares the same vibrational peaks. The elemental analysis presents that the DA of the isolated chitin remains similar to the commercial product about 84 - 88%. The Mw measurement results that the isolated chitin has 1068 × 103 g/mole and is close to the commercial chitin of 1156 × 103 g/mol. At the same time, the XRD, DSC, and SEM tests prove that the crystallinity degree, thermal property, and surface morphology of the isolated chitin are not much influenced by the ultrasonic treatment. Finally, the mechanism reaction of $CaCO_3$ demineralization is described with an appropriate kinetic model, in which reaction rate, $\frac{dCaCO_3}{dt} = -k_2 \frac{C_{H^+,0} C_{CaCO_3}}{(K_1 + C_{CaCO_3})}$, with reaction parameters:: first reaction order; $K_1 = 4.524.10^{-2}$; $A = 3.447.10^5$; and Ea = 359.289.

Declaration of Competing Interest

The authors declare that they have no known competing financial interests or personal relationships that could have appeared to influence the work reported in this paper.

The authors declare the following financial interests/personal relationships which may be considered as potential competing interests:

References

Ahyat, N.M., Mohamad, F., Ahmad, A., Azmi, A.A., 2017. Chitin and chitosan extraction from Portunus pelagicus. Malays. J. Anal. Sci. 21, 770–777.

Aktij, S.A., Taghipour, A., Rahimpour, A., Mollahosseini, A., Tiraferri, A., 2020. A critical review on ultrasonic-assisted fouling control and cleaning of fouled membranes. Ultrasonics 106228.
Alabaraoye, E., Achilonu, M., Hester, R., 2018. Biopolymer (Chitin) from various marine seashell wastes: isolation and characterization. J. Polym. Environ. 26, 2207–2218.
Alkhaldi, M.H., Nasr-El-Din, H.A., Sarma, H., 2010. Kinetics of the reaction of citric acid with calcite. SPE J. 15, 704–713.
Ashokkumar, M., 2011. The characterization of acoustic cavitation bubbles–an overview. Ultrason. Sonochem. 18, 864–872.
Baron, R., Socol, M., Arhaliass, A., Bruzac, S., Le Roux, K., Del Pino, J.R., Bergé, J.-.P., Kaas, R., 2015. Kinetic study of solid phase demineralization by weak acids in one-step enzymatic bio-refinery of shrimp cuticles. Process Biochem. 50, 2215–2223.
Borić, M., Vicente, F.A., Jurković, D.L., Novak, U., Likozar, B., 2020. Chitin isolation from crustacean waste using a hybrid demineralization/DBD plasma process. Carbohydrate. Polymers 246, 116648.
El Knidri, H., El Khalfaouy, R., Laajeb, A., Addaou, A., Lahsini, A., 2016. Eco-friendly extraction and characterization of chitin and chitosan from the shrimp shell waste via microwave irradiation. Process Saf. Environ. Prot. 104, 395–405.
Fusi, L., Monti, A., Primicerio, M., 2012. Determining calcium carbonate neutralization kinetics from experimental laboratory data. J. Math. Chem. 50, 2492–2511.
Gooday, G.W., 1990. The ecology of chitin degradation. Adv. Microbiol. Ecol. 387–430, 6.
Görgüç, A., Bircan, C., Yılmaz, F.M., 2019. Sesame bran as an unexploited by-product: effect of enzyme and ultrasound-assisted extraction on the recovery of protein and antioxidant compounds. Food Chem. 283, 637–645.
Hahn, T., Tafi, E., Paul, A., Salvia, R., Falabella, P., Zibek, S., 2020. Current state of chitin purification and chitosan production from insects. J. Chem. Technol. Biotechnol. 95, 2775–2795.
Hu, B., Guo, Y., Li, H., Liu, X., Fu, Y., Ding, F., 2021. Recent advances in chitosan-based layer-by-layer biomaterials and their biomedical applications. Carbohydr. Polym., 118427
Jovanović, J., Ćirković, J., Radojković, A., Mutavdžić, D., Tanasijević, G., Joksimović, K., Bakić, G., Branković, G., Branković, Z., 2021. Chitosan and pectin-based films and coatings with active components for application in antimicrobial food packaging. Prog. Org. Coat. 158, 106349.
Kaya, M., Mujtaba, M., Ehrlich, H., Salaberria, A.M., Baran, T., Amemiya, C.T., Galli, R., Akyuz, L., Sargin, I., Labidi, J., 2017. On chemistry of γ-chitin. Carbohydr. Polym. 176, 177–186.
Knidri, H.E., Dahmani, J., Addaou, A., Laajeb, A., Lahsini, A., 2019. Rapid and efficient extraction of chitin and chitosan for scale-up production: effect of process parameters on deacetylation degree and molecular weight. Int. J. Biol. Macromol. 139, 1092–1102.
Liu, S., Sun, J., Yu, L., Zhang, C., Bi, J., Zhu, F., Qu, M., Jiang, C., Yang, Q., 2012. Extraction and characterization of chitin from the beetle Holotrichia parallela Motschulsky. Molecules 17, 4604–4611.
Majekodunmi, S.O., 2016. Current development of extraction, characterization and evaluation of properties of chitosan and its use in medicine and pharmaceutical industry. Am. J. Polym. Sci. 6, 86–91.
Oyekunle, D.T., Omoleye, J.A., 2019. Effect of particle sizes on the kinetics of demineralization of snail shell for chitin synthesis using acetic acid. Heliyon 5, e02828.
Park, S., Baker, J.O., Himmel, M.E., Parilla, P.A., Johnson, D.K., 2010. Cellulose crystallinity index: measurement techniques and their impact on interpreting cellulase performance. Biotechnol. Biofuels 3, 10.
Patel, K., Panchal, N., Ingle, D.P., 2019. Review of extraction techniques. Int. J. Adv. Res. Chem. Sci. 6, 6–21.
Paul, T., Halder, S.K., Das, A., Ghosh, K., Mandal, A., Payra, P., Barman, P., Mohapatra, P.K.D., Pati, B.R., Mondal, K.C., 2015. Production of chitin and bioactive materials from Black tiger shrimp (Penaeus monodon) shell waste by the treatment of bacterial protease cocktail. 3 Biotech 5, 483–493.
Percot, A., Viton, C., Domard, A., 2003. Optimization of chitin extraction from shrimp shells. Biomacromolecules 4, 12–18.
Pereira, F.S., da Silva Agostini, D.L., Job, A.E., González, E.R.P., 2013. Thermal studies of chitin–chitosan derivatives. J. Therm. Anal. Calorim. 114, 321–327.
Peshkovsky, A.S., Peshkovsky, S.L., 2010. Acoustic Cavitation Theory and Equipment Design Principles For Industrial Applications of High-Intensity Ultrasound. Nova Science Publishers.
Pinem, M.P., Wardhono, E.Y., Nadaud, F., Clausse, D., Saleh, K., Guénin, E., 2020. Nanofluid to nanocomposite film: chitosan and cellulose-based edible packaging. Nanomaterials 10, 660.
Santos, V.P., Marques, N.S., Maia, P.C., Lima, M.A.B.de, Franco, L.de O., Campos-Takaki, G.M.de, 2020. Seafood waste as attractive source of chitin and chitosan production and their applications. Int. J. Mol. Sci. 21, 4290.
Ta, Q., Ting, J., Harwood, S., Browning, N., Simm, A., Ross, K., Olier, I., Al-Kassas, R., 2021. Chitosan nanoparticles for enhancing drugs and cosmetic components penetration through the skin. Eur. J. Pharm. Sci. 160, 105765.
Wang, J., Wang, Z., Vieira, C.L., Wolfson, J.M., Pingtian, G., Huang, S., 2019. Review on the treatment of organic pollutants in water by ultrasonic technology. Ultrason. Sonochem. 55, 273–278.
Wang, P., Li, L., Pang, X., Zhang, Yan, Zhang, Yang, Dong, W.-.F., Yan, R., 2021. Chitosan-Based Carbon Nanoparticles As a Heavy Metal Indicator and For Wastewater Treatment, 11. RSC Advanced, pp. 12015–12021.
Wardhono, E., Wahyudi, H., Agustina, S., Oudet, F., Pinem, M., Clausse, D., Saleh, K., Guénin, E., 2018. Ultrasonic irradiation coupled with microwave treatment for eco-friendly process of isolating bacterial cellulose nanocrystals. *Nanomaterials* 8, 859.
Wardhono, E.Y., Pinem, M.P., Kustiningsih, I., Agustina, S., Oudet, F., Lefebvre, C., Clausse, D., Saleh, K., Guénin, E., 2019. Cellulose nanocrystals to improve stability and functional properties of emulsified film based on chitosan nanoparticles and beeswax. Nanomaterials 9, 1707.
Wardhono, E.Y., Pinem, M.P., Kustiningsih, I., Effendy, M., Clausse, D., Saleh, K., Guénin, E., 2021. Heterogeneous deacetylation reaction of chitin under low-frequency ultrasonic irradiation. Carbohydr. Polym., 118180
Xu, J., McCarthy, S.P., Gross, R.A., Kaplan, D.L., 1996. Chitosan film acylation and effects on biodegradability. Macromolecules 29, 3436–3440.
Yao, Y., 2016. Enhancement of mass transfer by ultrasound: application to adsorbent regeneration and food drying/dehydration. Ultrason. Sonochem. 31, 512–531.
Yao, Y., Pan, Y., Liu, S., 2020. Power ultrasound and its applications: a state-of-the-art review. Ultrason. Sonochem. 62, 104722.
Younes, I., Rinaudo, M., 2015. Chitin and chitosan preparation from marine sources. Structure, properties and applications. Mar. Drugs 13, 1133–1174.
Zhang, K., Mao, Z., Huang, Y., Xu, Y., Huang, C., Guo, Y., Liu, C., 2020. Ultrasonic assisted water-in-oil emulsions encapsulating macro-molecular polysaccharide chitosan: influence of molecular properties, emulsion viscosity and their stability. Ultrason. Sonochem. 64, 105018.

Ultrasonic

ORIGINALITY REPORT

3%	0%	4%	4%
SIMILARITY INDEX	INTERNET SOURCES	PUBLICATIONS	STUDENT PAPERS

MATCHED SOURCE

1	Endarto Yudo Wardhono, Mekro Permana Pinem, Indar Kustiningsih, Mohammad Effendy et al. "Heterogeneous deacetylation reaction of chitin under low-frequency ultrasonic irradiation", Carbohydrate Polymers, 2021 Publication	3%

3%

★ Endarto Yudo Wardhono, Mekro Permana Pinem, Indar Kustiningsih, Mohammad Effendy et al. "Heterogeneous deacetylation reaction of chitin under low-frequency ultrasonic irradiation", Carbohydrate Polymers, 2021

Publication

Exclude quotes	Off	Exclude matches	< 3%
Exclude bibliography	On		

Ultrasonic

GRADEMARK REPORT

FINAL GRADE

/0

GENERAL COMMENTS

Instructor

PAGE 1

PAGE 2

PAGE 3

PAGE 4

PAGE 5

PAGE 6

PAGE 7

PAGE 8

PAGE 9

PAGE 10